RC23367 (W0410-054) October 8, 2004
Materials Science

IBM Research Report

Spalling of Intermetallic Compounds during the Reaction between Lead-free Solders and Electroless Ni-P Metallization

Y. C. Sohn, Jin Yu
Department of Materials Science and Engineering
Korea Advanced Institute of Science and Technology
373-1 Guseong-Dong, Yuseong-Gu, Daejeon 305-701
Korea

D. K. Kang, D. Y. Shih
IBM Research Division
Thomas J. Watson Research Center
P.O. Box 218
Yorktown Heights, NY 10598

T. Y. Lee
Department of Materials Science and Engineering
Hanbat National University
San 16-1, DukMyoung-Dong, Yuseong-Gu, Daejeon 305-764
Korea

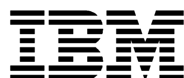

Research Division
Almaden - Austin - Beijing - Haifa - India - T. J. Watson - Tokyo - Zurich

LIMITED DISTRIBUTION NOTICE: This report has been submitted for publication outside of IBM and will probably be copyrighted if accepted for publication. It has been issued as a Research Report for early dissemination of its contents. In view of the transfer of copyright to the outside publisher, its distribution outside of IBM prior to publication should be limited to peer communications and specific requests. After outside publication, requests should be filled only by reprints or legally obtained copies of the article (e.g., payment of royalties). Copies may be requested from IBM T. J. Watson Research Center, P. O. Box 218, Yorktown Heights, NY 10598 USA (email: reports@us.ibm.com). Some reports are available on the internet at http://domino.watson.ibm.com/library/CyberDig.nsf/home

Spalling of Intermetallic Compounds During the Reaction Between Lead-free Solders and Electroless Ni-P Metallization

Y. C. Sohn (sonyc@kaist.ac.kr) and Jin Yu

Dept. of Materials Science and Engineering,

Korea Advanced Institute of Science and Technology

373-1 Guseong-Dong, Yuseong-Gu, Daejeon 305-701, Korea

S. K. Kang and D. Y. Shih

IBM T. J. Watson Research Center,

P.O.Box 218/Route 134, Yorktown Heights, NY 10598

T. Y. Lee

Dept. of Materials Science and Engineering, Hanbat National University,

San 16-1, DukMyoung-Dong, Yuseong-Gu, Deajeon 305-764, Korea

ABSTRACT

Intermetallic compound (IMC) spalling from electroless Ni-P film was investigated with lead-free solders (Sn-3.5 wt.% Ag and pure Sn) in terms of solder deposition methods (electroplating vs solder paste), P content in Ni-P layer (4.6, 9, and 13 wt.% P), and deposited solder thickness (120 and 200μm). The reaction of Ni-P with Sn3.5Ag paste easily led to IMC spalling after 2min reflow at 250°C while IMCs adhered to the Ni-P layer after 10min reflow for the reaction with electroplated Sn or Sn3.5Ag. It has shown that both solder composition and solder deposition method are important in determining IMC spalling from the Ni-P layer. The spalling increased with P content in the Ni-P layer as well as with solder volume. Ni_3Sn_4 intermetallics formed as a needle-shaped morphology in the early stage and changed into a chunky shape. Needle-shaped compounds exhibited a higher propensity for spalling from the Ni-P layer than chunky shaped compounds because molten solder can easily penetrate into the interface between needle shaped IMCs and the P-rich layer.

Key words : Pb-free solders, IMC Spalling, Intermetallic compounds, Ni-P

INTRODUCTION

Solder bumps in flip chip technologies of microelectronic devices is an interconnection for electrical data and thermal energy dissipation from an IC chip to a substrate.[1] The substrate in microelectronics packaging is usually made of organic PCB (Print Circuit Board), or LTCC (Low Temperature Cofired Ceramic).[2,3] The solder joint between an IC chip and a substrate is a key interconnection for the electrical performance and the reliability of an electronic system.

A reliable solder joint can be formed by a metallurgical reaction between a molten solder and under bump metallurgy (UBM) on a chip or metallization on a substrate, which produces stable intermetallic compounds (IMCs) at the joint interfaces.[4,5] Pb-containing solders have been extensively used in microelectronic interconnections. Recently, the industry is searching for Pb-free solders to replace Pb-containing solders for environmental reasons as well as consumers' desire on green products. Most of Pb-free solders are Sn-based alloys such as Sn-3.5%Ag, Sn-3.8%Ag-0.7%Cu, Sn-0.7%Cu (in wt.%) and others. The interfacial reactions between Pb-free solders and UBM have become a critical issue, because both the Sn content in the solders and their reflow temperatures are higher than the conventional Pb-Sn eutectic solder.[6-12] The previous studies on the interfacial reactions between high Sn solders and thin film UBM showed the IMC detachment or spalling. The IMC spalling can cause a reliability concern because it can result in dewetting of molten solder during joining and thereby yielding weak adhesion of solder joints during field operation. [13,14]

The spalling of Cu-Sn IMC from a chip was found during the reaction between eutectic SnPb solder and Cu-based UBM such as Ti/Cu, Cr/Cu/Au and phased-in Cr-Cu/Cu/Au. [15-17] In the case of Ti/Cu and Cr/Cu/Au UBM, the solder consumed all of the

Cu film and then IMCs were separated from the interface[15,16] because the compounds did not wet the adhesion layer such as Cr or Ti layer. The phased-in Cr-Cu UBM also failed in preventing the spalling of Cu_6Sn_5 formed in the eutectic SnPb while it prevented the spalling in the 95Pb5Sn solder.[17] A tensile and shear testing with Cr/Cu metallization and SnPb eutectic solder showed that the fracture strength decreased with annealing time due to IMC spalling from the Cr layer.[13] The spalling of Ni_3Sn_4 from Ni-based UBM (Ti/Ni) was also observed, eventually led to the dewetting of the molten solder from the Ti surface.[14] The thin film metallization of Al/Ni(V)/Cu, however, was reported to form stable Cu_6Sn_5 adhesion to Ni(V) without spalling during the reaction with eutectic SnPb .[18]

Reaction between Pb-free solders and Al/Ni(V)/Cu ball limiting metallization (BLM) showed different behaviors in reactions with eutectic SnPb and high Pb solders. In Sn-3.5Ag-1.0Cu, the Ni(V) layer was gradually dissolved into the molten solder during multiple reflow and the spalling of $(Cu,Ni)_6Sn_5$ IMC was observed.[7] In addition, the Ni metallizaton on the substrate side was reported to enhance dissolution of the interfacial IMC formed adjacent to the Ni(V) layer at the chip side.[8]

Recently, electroless Ni-P metallization has received great attention because of its low cost and the simple processing steps. The interfacial reactions between Pb-free solders and electroless Ni-P have been investigated.[9,10] The interfacial IMCs in the Sn-rich solders containing Cu such as 99.3Sn-0.7Cu and 95.5Sn-3.8Ag-0.7Cu had good adhesion with Ni-P while 96.5Sn-3.5Ag and 96Sn-2Ag-2Bi alloys formed needle-shaped IMCs that spalled off from the Ni-P layer.[9] IMC spalling on the Ni-P layer appears to be quite different from other metallizations. IMCs on Ni-P layer spall off before consuming all of the Ni-P layer, while IMCs from other metallizations usually spall off after consuming all

of the reaction layer. The previous studies on the reactions between Pb-free solders and Ni-P layer, however, had considered only the effect of solder composition. In this study, we have systematically investigated the IMC spalling behavior in Sn-rich, Pb-free solders from the Ni-P film in terms of solder deposition method, P content in Ni-P, reaction time and solder volume.

EXPERIMENTAL PROCEDURE

A Cu foil of 25μm thickness was used as a substrate, which was cleaned with acetone and treated in a 0.5M H_2SO_4 solution to remove surface oxides. The Cu foil was then activated with a Pd solution before electroless Ni-P plating. Ni-P films of 9μm thickness were electroless deposited for three different P contents (4.6, 9 and 13 wt.% P) with Technic EN 1400, EN 9185 and EN 3600 solutions (from Technic Inc, Cranston, RI), respectively, on the Cu foils.

The P content in a Ni-P layer was analyzed by an electron probe microanalyzer (EPMA). The microstructure of Ni-P is expected to vary depending on P content; nanocrystalline for 4.6 wt.% P, amorphous with some crystallites for 9 wt.% P, and completely amorphous for 13 wt.% P.[19-23]

Pure Sn and eutectic Sn-3.5Ag were used as solder materials in the present study. Two different Sn thickness, 120 and 200μm, were deposited on a Ni-P layer by electroplating with Solderon SC solution (from Shipley company, Marlborough, MA) with a current density of 37.5 mA/cm^2. A 120μm layer of Sn-3.5Ag was also deposited on a Ni-P layer by electroplating using UTB TS-140 solution (from Unicon Ishihara company, Japan) with 20 mA/cm^2. Sn-3.5Ag paste (from Heraeus Ltd.) was applied on a Ni-P layer

through a solder mask having an opening of 125μm diameter. And then, samples were reflowed for 1, 2 and 10min in a N_2 atmosphere to investigate IMC spalling and interfacial reactions between the Ni-P metallization and Pb-free solders.

To prepare a cross-sectional view, the reflowed samples were mounted with epoxy and then cross-sectioned metallographically. The samples were then etched with 3%HCl-5%HNO_3-92%CH_3OH (in vol%) solution for several minutes to reveal their microstructures. Scanning electron microscopy (SEM) with energy dispersive x-ray spectroscopy (EDX) was used for the microstructure and the composition analysis. The Ni-P films were denoted as Ni-4.6P, Ni-9P and Ni-13P specimens after their P weight percent in the films.

RESULTS

A. Effect of Solder Deposition Method

Fig. 1. shows two cross-sectional views of 9μm thick Ni-9P film reacted with Sn-3.5Ag paste (120μm thick) and electroplated Sn3.5Ag (120μm thick) after 10min reflow at 250°C. Ni_3Sn_4 IMC formed at the interface spalled off from the Ni-9P surface as shown in Fig. 1(a), while the Ni-Sn IMC formed at the interface of electroplated Sn3.5Ag adhered well to the Ni-P layer as shown in Fig 1(b). This is the first report to show all the IMCs well adhering to a Ni-P layer reacted with Pb-free solders without Cu after a long time reflow, such as 10min at 250°C. It was reported that Pb-free solders containing Cu such as Sn0.7Cu and Sn3.8Ag0.7Cu formed ternary Sn-Cu-Ni intermetallics and did not produce any IMC spalling from the Ni-P layer at the equivalent reflow condition.[9,10]

There are some differences between electroplated and paste solder. First, the initial

condition between solder and the Ni-P layer is different. For electroplated solder, before reflow, there would be chemical bonding between solder and the Ni-P metallization, but not for solder paste. Second, a solder paste is prepared as a mixture of metal powder and flux. For solder paste, the Ni-P surface would be in contact with the flux at early stage of reflow.

B. Effect of P Content on IMC Spalling

Fig. 2 shows the interfacial reactions as a function of P content (Ni-4.6P, Ni-9P and Ni-13P), reaction time (1 and 10 min) and two solder deposition methods (Sn-3.5Ag solder paste vs electroplated Sn with the same thickness, 120μm). For a short reacton of 1 min at 250°C and a low P content of 4.6%, Ni_3Sn_4 IMCs still adhered on the Ni-P layer, Fig. 2(a), but for the high P content, 13%, most IMCs spalled off from the Ni-P layer, Fig. 2(c). This indicates IMC spalling increases with the P content in the Ni-P layer. Meanwhile, for the electroplated Sn, IMCs (Ni_3Sn_4) adhered well on all the P content, even after 10 min reflow at 250°C as shown in Fig. 2(d), (e), and (f). Table 1 summarizes the spalling behaviors of Ni_3Sn_4 IMC from the Ni-P layer in terms of solder composition, deposition method, P content, solder thickness and reaction time.

A formation of Ni-Sn IMCs inside the solder matrix was also affected by the P content of the Ni-P layer; the IMCs were much longer and thicker in the high P samples as shown in Fig. 2(e) and (f). The formation of more Ni-Sn IMCs means that the dissolution of IMCs and metallization into the molten solder increases with P content. And it is also consistent with the trend of IMC spalling in Sn3.5Ag paste, where more spalling was observed with increasing P content.

In addition to P content, spalling of IMC is dependent on reflow time. For Sn3.5Ag

paste samples, IMC spalling was not observed for 1 min reflow time at 250°C, Fig. 2(a) and (b), but occurred for 10 min reflow as Fig. 1(a). For electroplated Sn and Sn3.5Ag samples, IMC spalling was not detected even after 10 min reflow.

C. Effect of Solder Volume

Fig. 3(a), (b) and (c) show SEM cross-sectional views of 9 μm thick Ni-9P film reacted with the electroplated Sn of two different thickness; 120 vs 200 μm. The morphology of Ni-Sn IMC and its spalling behavior were affected by the solder volume in contact with the Ni-P layer. With 120 μm solder, the IMC spalling was not observed even after 10 min reflow as shown in Fig. 2(e), while with 200 μm solder, the IMC spalling occurred after 10 min reflow at 250°C in Fig. 3(c). In addition, the IMC morphology has changed from the needle shape into a chunky shape in 120 μm solder after 10 min reflow, while this morphological change did not occur in 200 μm solder.

DISCUSSION

It is shown that IMC spalling from an electroless Ni-P layer is affected by P content, solder deposition method, and reaction time, while in case of electroplated Ni, it is not influenced by solder composition (or reaction time).[10] When a Ni-P film reacts with eutectic SnPb solder at the reflow temperature, a Ni_3P layer forms on top of the Ni-P layer while a Ni_3Sn_4 IMC forms simultaneously at the interface with the thickness ratio of Ni_3Sn_4 to Ni_3P being reported around 2.3~6.[24-26] In a eutectic SnAg or SnAgCu solder joint, a very thin nanocrystalline NiSnP layer was found between IMCs and the Ni_3P layer after the reflow process.[27,28] The adhesion and spalling of IMCs on the Ni-P layer

are expected to be critically dependent on the interface between IMCs and the NiSnP/Ni_3P layer in these Pb-free solders. For convenience, the NiSnP/Ni_3P layer is called as "P-rich layer" in this paper though the P content in the NiSnP layer was reported to be not higher than in the initial Ni-P layer.[27,28]

A. IMC Spalling Mechanism Based on Interfacial Energy

The IMC spalling behavior on the Ni-P surface, such as its dependence on P content and reaction time can be explained by considering the interfacial energies involved. From an interfacial energy consideration, a requirement for IMC spalling can be set as

$$\gamma_{np} > \gamma_{ps} + \gamma_{sn} \tag{1}$$

where γ_{np}, γ_{sn} and γ_{ps} be the interfacial energy of the interfaces of Ni_3Sn_4/P-rich layer, molten solder/Ni_3Sn_4 and P-rich layer/molten solder, respectively. From the previous works, the P-rich layer consists of a NiSnP layer on top of Ni_3P.[27,28] In additon, Kirkendall voids were found in the NiSnP layer between Ni_3P and IMCs. During the solid state aging at 170°C, voids become bigger and the composition of the NiSnP layer also changed.[27] From these results, it is reasonable to assume that the P-rich layer in our experiments would follow the similar trend during reflow process, i.e. the growth of voids and the change in the composition of P-rich layer. These changes would influence the interfacial energy of the IMC/P-rich layer, γ_{np}. In the early stage of reflow, equation (1) is not satisfied and IMCs are stable on the Ni-P layer. As the reflow time increases, γ_{np} increases to satisfy equation (1), which would result in IMC spalling.

The interfacial energy model can also explain the IMC spalling behavior as a function of P content. For a higher P content, the interfacial energy (γ_{np}) is expected to be larger

than a lower P content for a same reflow time. A different P content would also yield a different P composition in the P-rich layer and in turn change the interfacial energies.

The dependence of interfacial energy on the reaction and the composition at the interface is regarded to be quite different for the case of an electrolytic Ni UBM. Here the interfacial energy would remain unchanged until all the electrolytic Ni layer is consumed or it becomes thin enough for Sn atoms diffusing through to cause an appreciable change in the interfacial composition.

B. Spalling of Needle-Shaped IMCs

The interfacial IMCs (Ni_3Sn_4) initially form as a needle-shaped morphology as shown in Fig. 3(a) and (b). And they agglomerate into a chunky shape during the growth as shown in Fig. 2(d) and (e). The coarsening is a similar process to that of Cu_6Sn_5 compounds.[29] But Ni-Sn IMCs in some samples spalled off before they changed into a chunky morphology. Spalling was mainly found with the needle-shaped IMCs.

Fig. 4(a) shows a top view of Ni_3Sn_4 IMCs formed on 9μm thick Ni-4.6P layer reacted with 2μm thick Sn layer, which was heated up to 300°C.[30] The solder was completely etched away to reveal the needle-like morphology. Since equation (1) provides only a thermodynamic criterion for IMC spalling, a kinetic consideration should be given to explain fast spalling of needle-type IMCs. If we assume the IMC shape as a hexagonal column as depicted in Fig 4(b), the interfacial area can be roughly estimated for a needle-like vs chunky morphology by measuring the width of each IMC. As an example, the width of a needle is measured to be about 0.7μm in Fig. 3(a) and that of a chunky IMC is about 9μm in Fig. 2(e). The area ratio of a chunky IMC to a needle-type IMC is about 165. A large chunky IMC as shown in Fig. 2(e) is expected to replace more than 100

needle-like IMCs, even if some channels are considered among the IMCs. The change of needle-like IMCs into a chunky shape is therefore thermodynamically favorable since the large interfacial area between Ni_3Sn_4 needles and the molten solder can be eliminated. In addition, IMC spalling would complete when molten solder penetrates the interface between Ni_3Sn_4 and the P-rich layer, forming two interfaces; Ni_3Sn_4/solder and solder/P-rich layer. As reported in the study of the wetting reaction of molten solder on Cu [31], the channels among IMCs can provide paths for molten solder to penetrate the interface of Ni_3Sn_4/P-rich layer and finally to detach IMCs from the P-rich layer. The penetration length should be 10 times longer for the needle-like IMC in Fig. 3(a) than for the chunky one in Fig. 2(e) as depicted in Fig. 5. However, during the IMC coarsening occurs, the channel area for the supply of molten solder will dramatically decrease, by more than 100 times. Consequently, IMC spalling would be retarded.

CONCLUSIONS

IMC spalling was investigated for electroless Ni-P reacted with lead-free solders in terms of P content, solder volume, deposition method, and reaction time. From this study, the following conclusions are drawn:

1) The propensity for IMC spalling from an electroless Ni-P generally increases with increasing P content, solder volume, and reaction time.
2) The solder deposition method is important to determine the IMC spalling behavior; the solder deposited from solder paste has a higher tendency of IMC spalling than an electrodeposited solder under an equivalent reflow condition.
3) A thermodynamic criterion for IMC spalling has been proposed considering the

interfacial energies of individual interfaces formed between a molten solder and the Ni-P layer; the interfacial energies depend on reaction time and the composition at the interface.

4) The morphology of Ni-Sn IMCs is found to influence their spalling behavior; a needle-like morphology is more prone to spalling in comparison with a chunky morphology. The fast spalling of needle-like IMCs has been explained by considering the reaction kinetic factor such as channels among the needle-like IMCs.

Acknowledgements

This work was supported by the Center for Electronic Packaging Materials of Korea Science and Engineering Foundation.

References

1. Rao R. Tummala, Eugene J. Rymaszewski and Alan G. Klopfenstein (ed), Microelectronics Packaging Handbook, 2nd edition, Part2, Ch8, p.---,, Chapman & Hall, 1997
2. M. Baker-Pole. “Printed circuits-Origin and Development, Part2”, Circuit World **10(3)**, 8 (1984).
3. Y. Shimade, K. Utsumi, M. Suzuki, H. Takamizowa, M. Nitta and T. Watari. “low firing temperature multiplayer glass-ceramic substrate” IEEE Trans. Components, Hybrids Manuf. Technol., CHMT **6(4)** 382 (1983).

4. S. K. Kang and V. Ramachandran, Scripta Met, **14(4)**, 421 (1980)
5. G. A. Walker and P. W. Dehaven and C. C. Goldsmith, Proceedings of IEEE Electronic Component and Technology Conference, 1984, p. 125.
6. S. K. Kang, R. S. Rai and S. Purushothaman, J. Electron. Mater. **25(7)**, 1113 (1996).
7. M. Li, F. Zhang, W. T. Chen, K. Zeng, K. N. Tu, H. Balkan and P. Elenius, J. Mater. Res. **17**, 1612 (2002).
8. F. Zhang, M. Li, C. C. Chum and K. N. Tu, J. Mater. Res. **17**, 2757 (2002).
9. J. W. Jang, D. R. Frear, T. Y. Lee and K. N. Tu, J. Appl. Phys. **88**, 6359 (2000).
10. S. K. Kang, D. Y. Shih, K. Fogel, P. Lauro, M. J. Yim, G. Advocate, M. Griffin, C. Goldsmith, D. W. Henderson, T. Gosselin, D. King, J. Konrad, A. Sarkhel and K. J. Puttlitz, Proceedings of IEEE Electronic Component and Technology Conference, 2001, p. 448.
11. G. Ghosh, Acta mater. **49**, 2609 (2001).
12. M. O. Alam, Y. C. Chan and K. C. Hung, Proceedings of IEEE Electronic Component and Technology Conference, 2002, p. 1650.
13. C. Y. Liu, Chih Chen, A. K. Mal and K. N. Tu, J. Appl. Phys. **85**, 3882 (1999).
14. P. G. Kim, J. W. Jang, T. Y. Lee and K. N. Tu, J. Appl. Phys. **86**, 6746 (1999).
15. H. K. Kim, K. N. Tu and P. A. Totta, Appl. Phys. Lett. **68**, 2204 (1996).
16. Ann A. Liu, H. K. Kim, K. N. Tu and P. A. Totta, J. Appl. Phys. **80**, 2774 (1996).
17. G. Z. Pan, Ann A. Liu, H. K. Kim, K. N. Tu and P. A. Totta, Appl. Phys. Lett. **71**, 2946 (1997).
18. C. Y. Liu, K. N. Tu, T. T. Sheng, C. H. Tung, D. R. Frear and P. Elenius, J. Appl. Phys. **87**, 750 (2000).

19. Kreye, H., Müller, F., Lang, K., Isheim, D. and Hentschel, T., Z. Metallkd. **86**, 184 (1995).
20. Kreye, H., Müller, H.-H. and Petzel, T., Galvanotechnik **77**, 561 (1986).
21. Dietz, G. and Schneider, H. D., J. Phys.: Condens. Matter **2**, 2169 (1990).
22. S. H. Park and D. N. Lee, J. Mater. Sci. **23**, 1643 (1988).
23. K. H. Hur, J. H. Jeong and D. N. Lee, J. Mater. Sci. **25**, 2573 (1990).
24. J. W. Jang, P. G. Kim, K. N. Tu, D. R. Frear and P. Thompson, J. Appl. Phys. **85**, 8456 (1999).
25. K. C. Hung, Y. C. Chan, C. W. Tang and H. C. Ong, J. Mater. Res. **15**, 2534 (2000).
26. Y. C. Sohn, Jin Yu, S. K. Kang, W. K. Choi and D. Y. Shih, J. Mater. Res. **18**, 4 (2003).
27. K. Zeng and K. N. Tu, Mater. Sci. and Eng. **R38**, 55 (2002).
28. M. Ito, M. Yoshikawa, Y. Tanii, T. Ito, Y. Nakagawa, G. Katagiri, T. Hiramori, A. Hirose and K. F. Kobayashi, Proceedings of International Conference on Electronics Packaging, 2003, p.254.
29. H. K. Kim and K. N. Tu, Phys. Rev. **B53**, 16027 (1996).
30. Y. C. Sohn, Jin Yu, S. K. Kang, W. K. Choi and D. Y. Shih, accepted to J. Electron. Mater.
31. K. N. Tu and K. Zeng, Mater. Sci. and Eng. **R34**, 1 (2001).

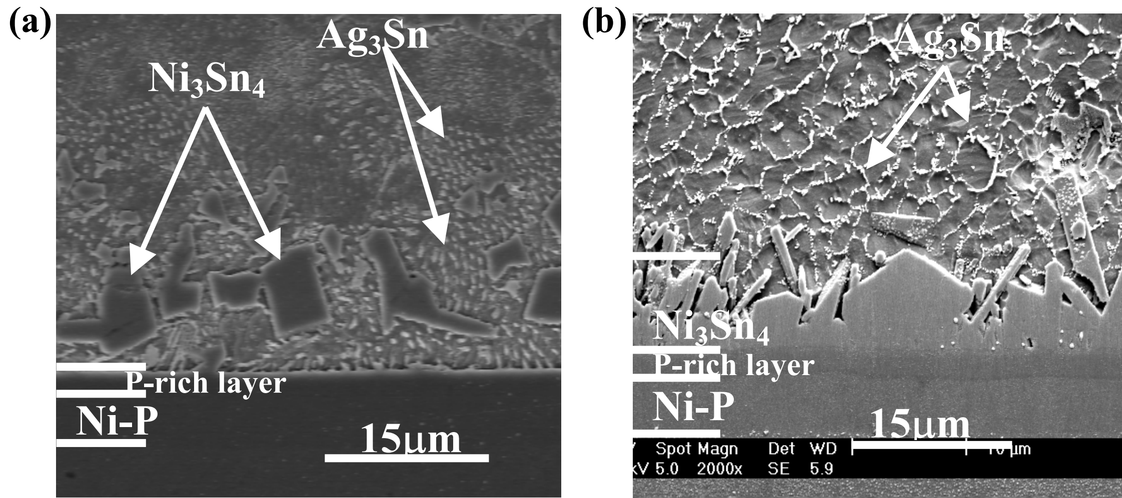

Fig. 1. Cross-sectional SEM micrographs of 9μm thick Ni-9P reacted with (a) 120μm thick Sn3.5Ag paste and (b) 120μm thick electroplated Sn3.5Ag after 10min reflow at 250°C.

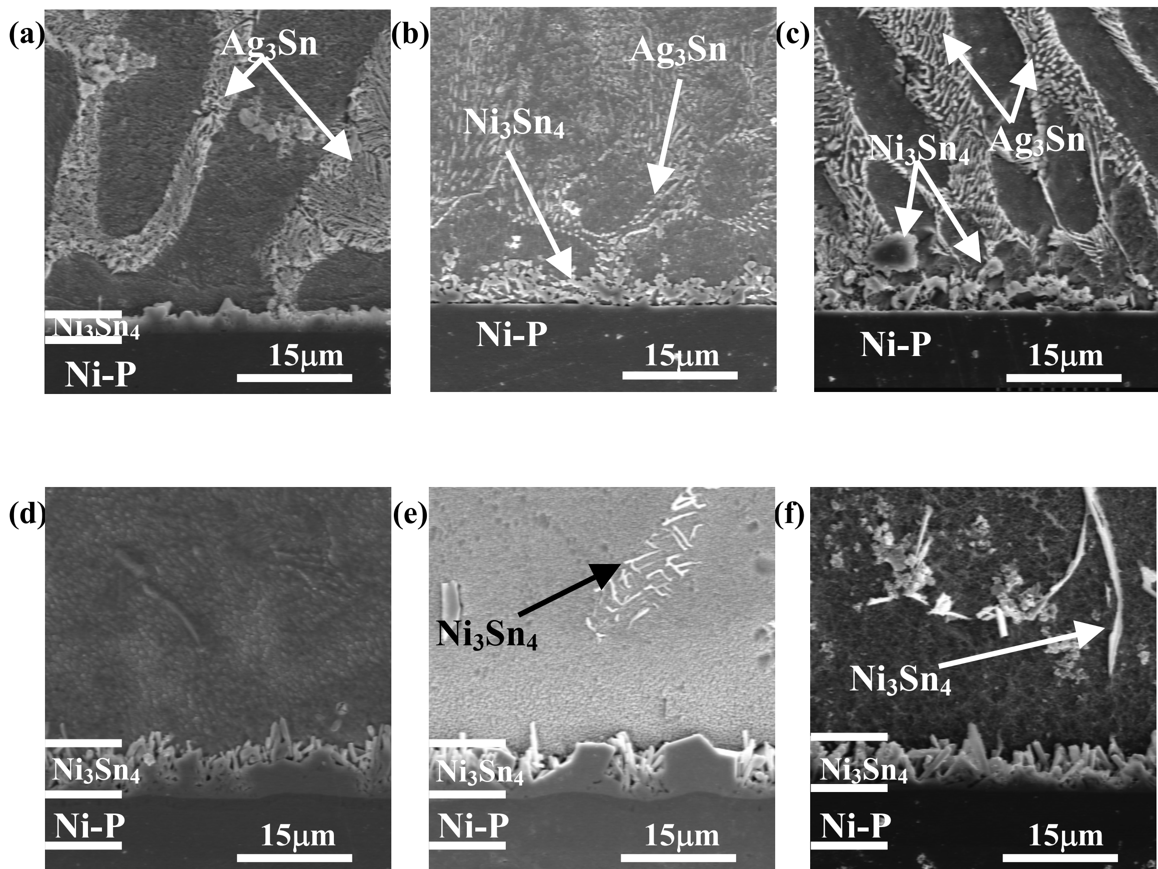

Fig. 2. Cross-sectional SEM micrographs of 9μm thick (a) Ni-4.6P, (b) Ni-9P and (c) Ni-13P reacted with 120μm thick Sn3.5Ag paste after 1min reflow at 250°C and 9μm thick (d) Ni-4.6P, (e) Ni-9P and (f) Ni-13P reacted with 120μm thick electroplated Sn after 10min reflow at 250°C.

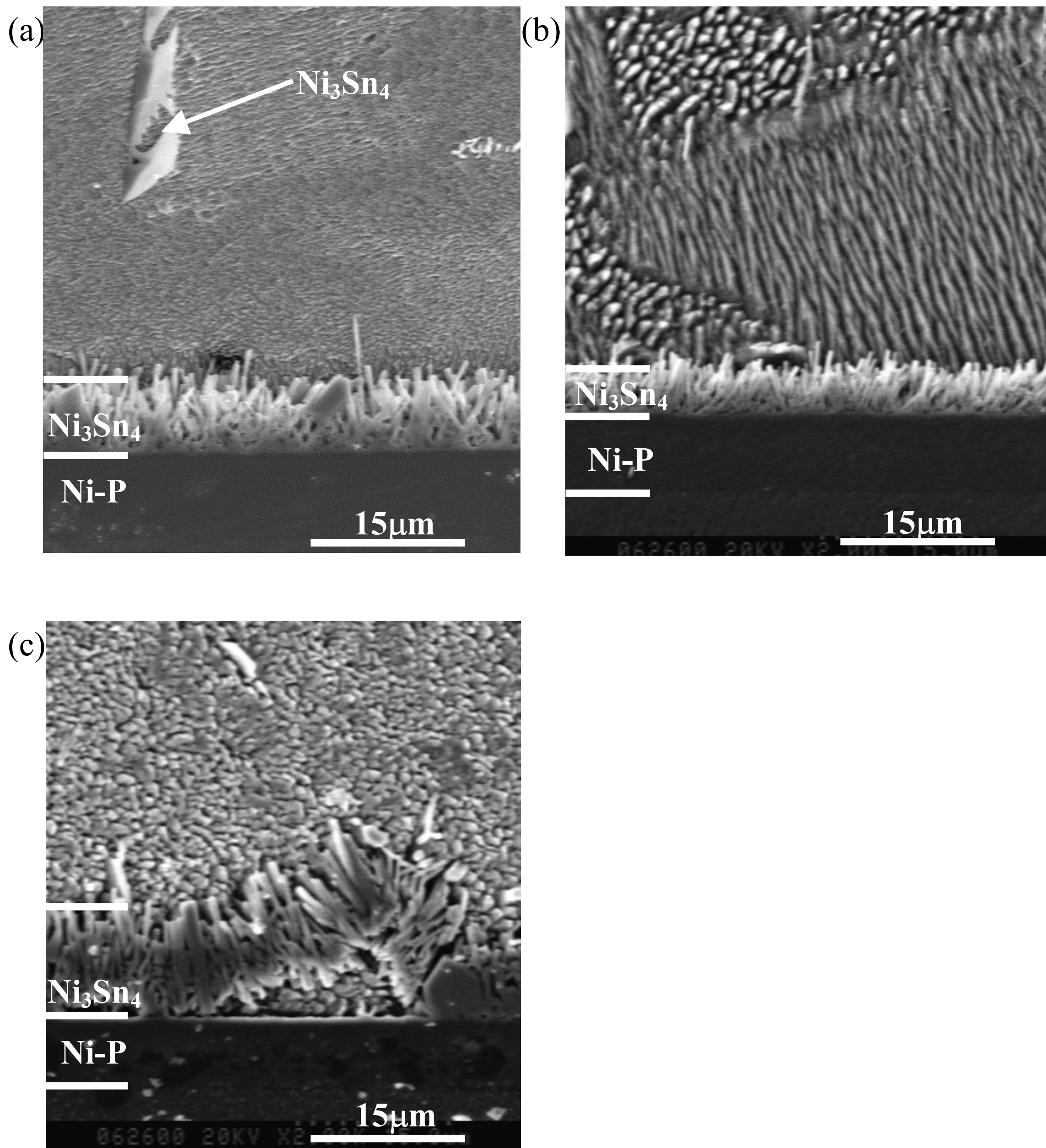

Fig. 3. Cross-sectional SEM micrographs of (a) 9μm thick Ni-9P layer reacted with 120μm thick electroplated Sn after 2min reflow, (b) 9μm thick Ni-9P layer reacted with 200μm thick electroplated Sn after 2min reflow and (c) after 10 min reflow at 250°C.

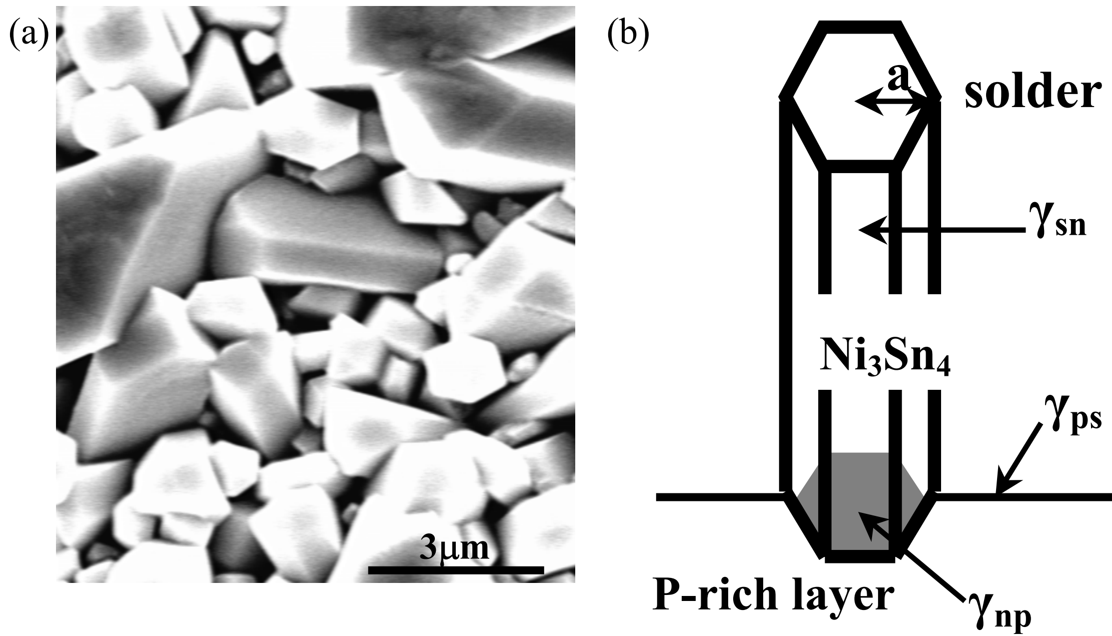

Fig. 4. (a) Top morphology of Ni_3Sn_4 formed on 9μm thick Ni-4.6P layer with 2μm thick electroplated Sn heated up to 300°C at a heating rate of 5°C/min and (b) a schematic diagram depicting column-like Ni_3Sn_4 on the P-rich layer.

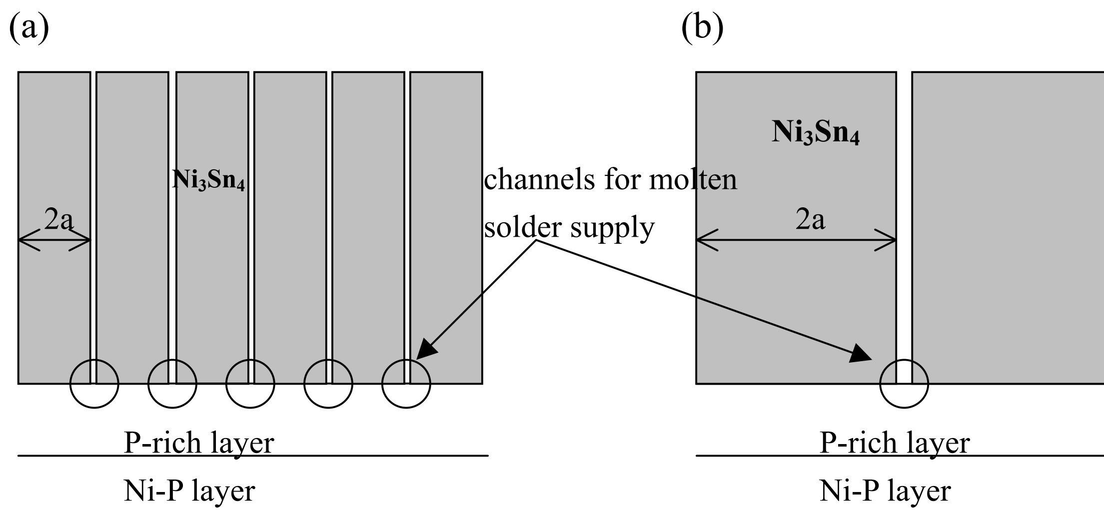

Fig. 5. Schematic diagrams depicting channels (a) among needle shaped IMCs and (b) among chunk shaped IMCs. (The diagrams are not scaled.)

Table 1. Morphology and spalling behavior of Ni_3Sn_4 compounds.

P content in Ni-P	solder	deposition method	thickness (μm)	reflow (min)	IMC morphology at the interface	spalling
4.6 wt.%	Sn3.5Ag	paste	120	1	needle	none
				2	N.D.	partially
				10	N.D.	mostly
	Sn	plating	120	1	needle	none
				2	needle>chunk	none
				10	chunk>needle	none
9 wt.%	Sn3.5Ag	paste	120	1	needle	partially
				2	N.D.	mostly
				10	N.D.	mostly
		plating	120	2	needle>chunk	none
				10	chunk>needle	none
	Sn	plating	120	1	needle	none
				2	needle>chunk	none
				10	chunk>needle	none
			200	2	needle	partially
				10	needle	partially
13 wt.%	Sn3.5Ag	paste	120	1	N.D.	mostly
				2	N.D.	mostly
				10	N.D.	mostly
	Sn	plating	120	2	needle	none
				10	needle	none

N.D. : not determined